

Strange anti-particle to particle ratios at mid-rapidity in

$$\sqrt{s_{NN}} = 130 \text{ GeV Au+Au Collisions}$$

J. Adams,³ C. Adler,¹¹ Z. Ahammed,²³ C. Allgower,¹² J. Amonett,¹⁴ B.D. Anderson,¹⁴ M. Anderson,⁵ G.S. Averichev,⁹ J. Balewski,¹² O. Barannikova,^{23,9} L.S. Barnby,^{14,*} J. Baudot,¹³ S. Bekele,²⁰ V.V. Belaga,⁹ R. Bellwied,³¹ J. Berger,¹¹ H. Bichsel,³⁰ A. Billmeier,³¹ L.C. Bland,² C.O. Blyth,³ B.E. Bonner,²⁴ A. Boucham,²⁶ A. Brandin,¹⁸ A. Bravar,² R.V. Cadman,¹ H. Caines,³³ M. Calderón de la Barca Sánchez,² A. Cardenas,²³ J. Carroll,¹⁵ J. Castillo,¹⁵ M. Castro,³¹ D. Cebra,⁵ P. Chaloupka,²⁰ S. Chattopadhyay,³¹ Y. Chen,⁶ S.P. Chernenko,⁹ M. Cherney,⁸ A. Chikhanian,³³ B. Choi,²⁸ W. Christie,² J.P. Coffin,¹³ T.M. Cormier,³¹ M.M. Corral,¹⁶ J.G. Cramer,³⁰ H.J. Crawford,⁴ W.S. Deng,¹⁴ A.A. Derevschikov,²² L. Didenko,² T. Dietel,¹¹ J.E. Draper,⁵ V.B. Dunin,⁹ J.C. Dunlop,³³ V. Eckardt,¹⁶ L.G. Efimov,⁹ V. Emelianov,¹⁸ J. Engelage,⁴ G. Eppley,²⁴ B. Erazmus,²⁶ P. Fachini,² V. Faine,² J. Faivre,¹³ R. Fatemi,¹² K. Filimonov,¹⁵ E. Finch,³³ Y. Fisyak,² D. Flierl,¹¹ K.J. Foley,² J. Fu,^{15,32} C.A. Gagliardi,²⁷ N. Gagunashvili,⁹ J. Gans,³³ L. Gaudichet,²⁶ M. Germain,¹³ F. Geurts,²⁴ V. Ghazikhanian,⁶ O. Grachov,³¹ V. Grigoriev,¹⁸ M. Guedon,¹³ S.M. Guertin,⁶ E. Gushin,¹⁸ T.J. Hallman,² D. Hardtke,¹⁵ J.W. Harris,³³ M. Heinz,³³ T.W. Henry,²⁷ S. Heppelmann,²¹ T. Herston,²³ B. Hippolyte,¹³ A. Hirsch,²³ E. Hjort,¹⁵ G.W. Hoffmann,²⁸ M. Horsley,³³ H.Z. Huang,⁶ T.J. Humanic,²⁰ G. Igo,⁶ A. Ishihara,²⁸ Yu.I. Ivanshin,¹⁰ P. Jacobs,¹⁵ W.W. Jacobs,¹² M. Janik,²⁹ I. Johnson,¹⁵ P.G. Jones,³ E.G. Judd,⁴ M. Kaneta,¹⁵ M. Kaplan,⁷ D. Keane,¹⁴ J. Kiryluk,⁶ A. Kisiel,²⁹ J. Klay,¹⁵ S.R. Klein,¹⁵ A. Klyachko,¹² T. Kollegger,¹¹ A.S. Konstantinov,²² M. Kopytine,¹⁴ L. Kotchenda,¹⁸ A.D. Kovalenko,⁹ M. Kramer,¹⁹ P. Kravtsov,¹⁸ K. Krueger,¹ C. Kuhn,¹³ A.I. Kulikov,⁹ G.J. Kunde,³³ C.L. Kunz,⁷ R.Kh. Kutuev,¹⁰ A.A. Kuznetsov,⁹ M.A.C. Lamont,³ J.M. Landgraf,² S. Lange,¹¹ C.P. Lansdell,²⁸ B. Lasiuk,³³ F. Laue,² J. Lauret,² A. Lebedev,² R. Lednický,⁹ V.M. Leontiev,²² M.J. LeVine,² Q. Li,³¹ S.J. Lindenbaum,¹⁹ M.A. Lisa,²⁰ F. Liu,³² L. Liu,³² Z. Liu,³² Q.J. Liu,³⁰ T. Ljubicic,² W.J. Llope,²⁴ H. Long,⁶ R.S. Longacre,² M. Lopez-Noriega,²⁰ W.A. Love,² T. Ludlam,² D. Lynn,² J. Ma,⁶ D. Magestro,²⁰ R. Majka,³³ S. Margetis,¹⁴ C. Markert,³³ L. Martin,²⁶ J. Marx,¹⁵ H.S. Matis,¹⁵ Yu.A. Matulenko,²² T.S. McShane,⁸ F. Meissner,¹⁵ Yu. Melnick,²² A. Meschanin,²² M. Messer,² M.L. Miller,³³ Z. Milosevich,⁷ N.G. Minaev,²² J. Mitchell,²⁴ C.F. Moore,²⁸ V. Morozov,¹⁵ M.M. de Moura,³¹ M.G. Munhoz,²⁵ J.M. Nelson,³ P. Nevski,² V.A. Nikitin,¹⁰ L.V. Nogach,²² B. Norman,¹⁴ S.B. Nurushev,²² G. Odyniec,¹⁵ A. Ogawa,² V. Okorokov,¹⁸ M. Oldenburg,¹⁶ D. Olson,¹⁵ G. Paic,²⁰ S.U. Pandey,³¹ Y. Panebratsev,⁹ S.Y. Panitkin,² A.I. Pavlinov,³¹ T. Pawlak,²⁹ V. Perevoztchikov,² W. Peryt,²⁹ V.A. Petrov,¹⁰ M. Planinic,¹² J. Pluta,²⁹ N. Porile,²³ J. Porter,² A.M. Poskanzer,¹⁵ E. Potrebenikova,⁹ D. Prindle,³⁰ C. Pruneau,³¹ J. Putschke,¹⁶ G. Rai,¹⁵ G. Rakness,¹² O. Ravel,²⁶ R.L. Ray,²⁸ S.V. Razin,^{9,12} D. Reichhold,²³ J.G. Reid,³⁰ G. Renault,²⁶ F. Retiere,¹⁵ A. Ridiger,¹⁸ H.G. Ritter,¹⁵ J.B. Roberts,²⁴ O.V. Rogachevski,⁹ J.L. Romero,⁵ A. Rose,³¹ C. Roy,²⁶ V. Rykov,³¹ I. Sakrejda,¹⁵ S. Salur,³³ J. Sandweiss,³³ I. Savin,¹⁰ J. Schambach,²⁸ R.P. Scharenberg,²³ N. Schmitz,¹⁶ L.S. Schroeder,¹⁵ A. Schüttauf,¹⁶ K. Schweda,¹⁵ J. Seger,⁸ D. Seliverstov,¹⁸ P. Seyboth,¹⁶ E. Shahaliev,⁹ K.E. Shestermanov,²² S.S. Shimanskii,⁹ F. Simon,¹⁶ G. Skoro,⁹ N. Smirnov,³³ R. Snellings,¹⁵ P. Sorensen,⁶ J. Sowinski,¹² H.M. Spinka,¹ B. Srivastava,²³ E.J. Stephenson,¹² R. Stock,¹¹ A. Stolpovsky,³¹ M. Strikhanov,¹⁸ B. Stringfellow,²³ C. Struck,¹¹ A.A.P. Suaide,³¹ E. Sugarbaker,²⁰ C. Suire,² M. Šumbera,²⁰ B. Surrow,² T.J.M. Symons,¹⁵ A. Szanto de Toledo,²⁵ P. Szarwas,²⁹ A. Tai,⁶ J. Takahashi,²⁵ A.H. Tang,¹⁵ D. Thein,⁶ J.H. Thomas,¹⁵ M. Thompson,³ V. Tikhomirov,¹⁸ M. Tokarev,⁹ M.B. Tonjes,¹⁷ T.A. Trainor,³⁰ S. Trentalange,⁶ R.E. Tribble,²⁷ V. Trofimov,¹⁸ O. Tsai,⁶ T. Ullrich,² D.G. Underwood,¹ G. Van Buren,² A.M. VanderMolen,¹⁷ I.M. Vasilevski,¹⁰ A.N. Vasiliev,²² S.E. Vigdor,¹² S.A. Voloshin,³¹ F. Wang,²³ H. Ward,²⁸ J.W. Watson,¹⁴ R. Wells,²⁰ G.D. Westfall,¹⁷ C. Whitten Jr.,⁶ H. Wieman,¹⁵ R. Willson,²⁰ S.W. Wissink,¹² R. Witt,³³ J. Wood,⁶ N. Xu,¹⁵ Z. Xu,² A.E. Yakutin,²² E. Yamamoto,¹⁵ J. Yang,⁶ P. Yepes,²⁴ V.I. Yurevich,⁹ Y.V. Zanevski,⁹ I. Zborovský,⁹ H. Zhang,³³ W.M. Zhang,¹⁴ R. Zoulkarneev,¹⁰ and A.N. Zubarev⁹

(STAR Collaboration)[†]

¹Argonne National Laboratory, Argonne, Illinois 60439

²Brookhaven National Laboratory, Upton, New York 11973

³University of Birmingham, Birmingham, United Kingdom

⁴University of California, Berkeley, California 94720

⁵University of California, Davis, California 95616

⁶University of California, Los Angeles, California 90095

⁷Carnegie Mellon University, Pittsburgh, Pennsylvania 15213

⁸Creighton University, Omaha, Nebraska 68178

⁹Laboratory for High Energy (JINR), Dubna, Russia

¹⁰Particle Physics Laboratory (JINR), Dubna, Russia

- ¹¹University of Frankfurt, Frankfurt, Germany
¹²Indiana University, Bloomington, Indiana 47408
¹³Institut de Recherches Subatomiques, Strasbourg, France
¹⁴Kent State University, Kent, Ohio 44242
¹⁵Lawrence Berkeley National Laboratory, Berkeley, California 94720
¹⁶Max-Planck-Institut fuer Physik, Munich, Germany
¹⁷Michigan State University, East Lansing, Michigan 48824
¹⁸Moscow Engineering Physics Institute, Moscow Russia
¹⁹City College of New York, New York City, New York 10031
²⁰Ohio State University, Columbus, Ohio 43210
²¹Pennsylvania State University, University Park, Pennsylvania 16802
²²Institute of High Energy Physics, Protvino, Russia
²³Purdue University, West Lafayette, Indiana 47907
²⁴Rice University, Houston, Texas 77251
²⁵Universidade de Sao Paulo, Sao Paulo, Brazil
²⁶SUBATECH, Nantes, France
²⁷Texas A & M, College Station, Texas 77843
²⁸University of Texas, Austin, Texas 78712
²⁹Warsaw University of Technology, Warsaw, Poland
³⁰University of Washington, Seattle, Washington 98195
³¹Wayne State University, Detroit, Michigan 48201
³²Institute of Particle Physics, CCNU (HZNU), Wuhan, 430079 China
³³Yale University, New Haven, Connecticut 06520

(Dated: October 30, 2018)

Values of the ratios in the mid-rapidity yields of $\bar{\Lambda}/\Lambda = 0.71 \pm 0.01(stat.) \pm 0.04(sys.)$, $\bar{\Xi}^+/\Xi^- = 0.83 \pm 0.04(stat.) \pm 0.05(sys.)$, $\bar{\Omega}^+/\Omega^- = 0.95 \pm 0.15(stat.) \pm 0.05(sys.)$ and $K^+/K^- = 1.092 \pm 0.023(combined)$ were obtained in central $\sqrt{s_{NN}} = 130$ GeV Au+Au collisions using the STAR detector. The ratios indicate that a fraction of the net-baryon number from the initial system is present in the excess of hyperons over anti-hyperons at mid-rapidity. The trend in the progression of the baryon ratios, with increasing strange quark content, is similar to that observed in heavy-ion collisions at lower energies. The value of these ratios may be related to the charged kaon ratio in the framework of simple quark-counting and thermal models.

PACS numbers: 25.75.Dw

Keywords: relativistic heavy-ion collisions; anti-baryon to baryon ratios; baryochemical potential; strangeness; STAR

The goal of the experimental program at the Relativistic Heavy Ion Collider (RHIC) is to study new states of nuclear matter which have been predicted to form in heavy-ion collisions [1, 2] and for which much indirect evidence has emerged from a previous series of experiments at lower energy [3, 4, 5, 6, 7, 8, 9, 10, 11]. Measurements of anti-particle to particle ratios in these collisions give information on the net baryon density or baryochemical potential achieved [12] and are thus of interest in characterizing the environment created in these collisions. It has also been suggested that the measurement of strange anti-baryon to baryon ratios could help distinguish between a hadron gas and a deconfined plasma of quarks and gluons [13]. The dominant production mechanism for anti-quarks is via gluon fusion [14, 15] and a measurement of the anti-baryon to baryon ratio therefore probes the gluonic degrees of freedom. The relations between the various anti-particle to particle ratios allow for the test

of a non-linear quark coalescence model [16, 17] which is consistent with the existence of quark degrees of freedom. We present here the first measurements of multi-strange baryon production at $\sqrt{s_{NN}} = 130$ GeV and utilize recently revised \bar{p}/p [32] and published $\bar{\Lambda}/\Lambda$ [26] results to compare to models.

The Solenoidal Tracker at RHIC (STAR) detector system [18], in the configuration used to collect the data presented here, consisted principally of a large cylindrical Time Projection Chamber (TPC) used for charged particle tracking. The TPC has inner and outer radii of 50 cm and 200 cm respectively, a total length of approximately 420 cm and was operated in a 0.25 Tesla magnetic field. It is surrounded by a cylinder of scintillator slats forming a Central Trigger Barrel (CTB), a fast detector providing a signal proportional to the multiplicity within pseudo-rapidity ± 1 . Two Zero Degree Calorimeters (ZDCs) were used to detect spectator neutrons from the colliding ions at close to beam rapidities [19]. Collisions were triggered by requiring coincident signals in the ZDCs which formed a minimum bias trigger. Approximately 250,000 of these events were used in the analysis. An enriched central data sample was acquired, with the

*Electronic address: lbarnby@bnl.gov

†URL: www.star.bnl.gov

additional requirement of a high CTB threshold, corresponding approximately to the 14% most central events. On these events a further centrality selection was made off-line, by cutting on the observed track multiplicity in the TPC after event reconstruction. This analysis used approximately 180,000 central $\sqrt{s_{NN}} = 130$ GeV Au+Au events after the multiplicity cut, corresponding to the most central 11% of the total hadronic cross-section [20].

Two techniques were used to extract the raw yields of strange particles. First, charged kaons were identified via their specific ionization, or energy loss (dE/dx), in the TPC. Second, these and other strange particles were reconstructed from their decay topology.

Up to 45 ionization samples were measured for each track. The dE/dx resolution was measured to be 11% following the procedure of [21]. For the charged kaon dE/dx analysis only tracks below a momentum of 0.6 GeV/ c were used, where the dE/dx of kaons is distinct from those of other particle species. In addition, tracks were required to originate from the primary interaction vertex within 3 cm. Similar to [22], the distribution of $Z = \log[(dE/dx)_{Meas}/(dE/dx)_{BB}]$, where $(dE/dx)_{BB}$ is the dE/dx from a Bethe-Bloch parameterization, is fitted with a convolution of Gaussian functions. The kaon raw yields were extracted from the fit results for each p_T bin within rapidity $|y| < 0.4$.

The most versatile technique for the reconstruction of strange particles is via their decay topologies [23]. The decay $\Lambda \rightarrow p\pi^-$ (64% branching ratio) and the charge conjugate decay for $\bar{\Lambda}$ result in two charged particles in the final state. The Λ particles from the electromagnetic decay of the Σ^0 are included in the Λ sample since they were not experimentally distinguishable from the primary Λ population. The momenta of these charged daughter particles are calculated from their trajectories in the TPC. Both tracks can be extrapolated back toward the primary interaction vertex to locate their common point of origin, where the kinematic properties of the parent can be calculated. In this process, all pairs of positively and negatively charged tracks in an event are considered. To reduce the large combinatorial background which results from random crossings of tracks interior to the TPC fiducial volume, additional cuts must be made. The most important criteria for improving the signal to noise ratio are that the decay vertex is well separated from the primary interaction and that the parent originates from the primary interaction vertex while the daughters do not. An additional requirement that the dE/dx of the daughters is compatible with the expected decay mode is also applied. For example the positively charged daughter of a Λ should have a dE/dx compatible with it being a proton. This helps to suppress the background from fake decays with two pion daughter particles with $p \lesssim 1$ GeV/ c . This technique is extended to enable the reconstruction of the $\Xi^- \rightarrow \Lambda\pi^-$ and $\Omega^- \rightarrow \Lambda K^-$ decays (100% and 68% branching ratios respectively) and their charge conjugate $\bar{\Xi}^+$ and $\bar{\Omega}^+$ decays. Here, only Λ (or $\bar{\Lambda}$) candidates within ± 7 MeV/ c^2 of the expected

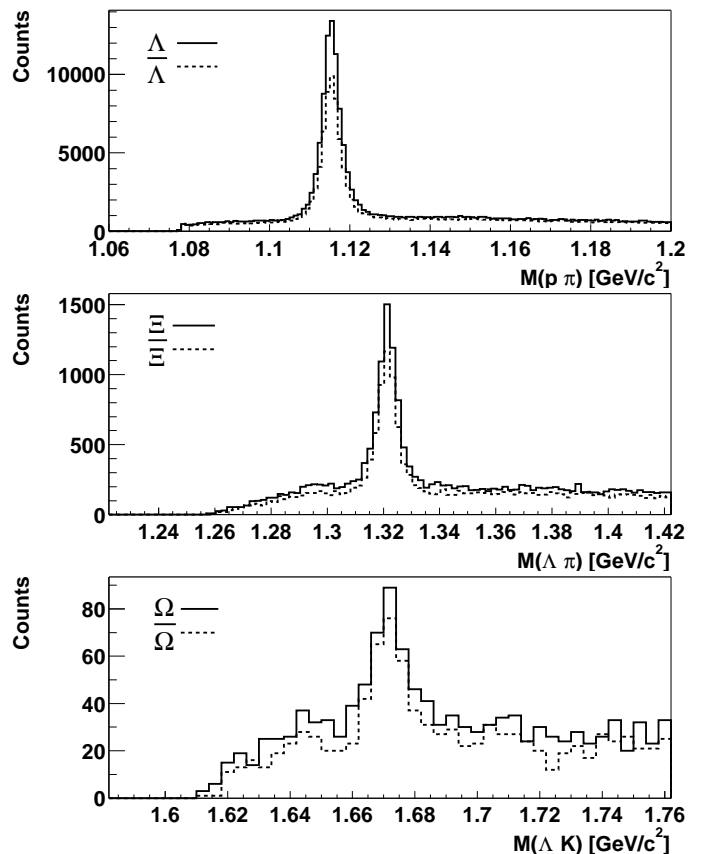


FIG. 1: Invariant mass distributions for $p\pi^-$ and $\bar{p}\pi^+$ (top panel), $\Lambda\pi^-$ and $\bar{\Lambda}\pi^+$ (middle panel) and ΛK^- and $\bar{\Lambda}K^+$ (lower panel).

mass [24] are used and the requirement that the Λ (or $\bar{\Lambda}$) originates from the primary interaction vertex is relaxed. The resulting invariant mass distributions for Λ , Ξ^- and Ω^- , with their anti-particle distributions superimposed, are shown in Figure 1. The remaining background under the peak in each invariant mass distribution was subtracted by using a linear interpolation between the background regions a few MeV/ c^2 on either side of the peak region.

Charged kaons can also be reconstructed using a variation on this topological technique via their one-prong decay channels. The most prominent of these are $K \rightarrow \mu\nu$ and $K \rightarrow \pi\pi^0$, with 64% and 21% branching ratios, respectively. In this “kink” method the tracks from the charged kaon and charged daughter particle are used to reconstruct the kinematics of the decay. In order that both parent and daughter are reconstructed in the TPC with good momentum resolution, the fiducial volume for the location of the decay vertex is restricted to radii of 130 – 180 cm. The background comes from charged pion decays, multiple scattering and hadronic interactions in the TPC gas and combinatorics. The pion decay contribution can be largely eliminated by a cut on the opening angle between the parent and daughter tracks. This angle, for a given momentum, is much smaller for a pion

decay than a kaon decay. The remaining background level was estimated to be approximately 15% [25]. The method allows charged kaons to be identified over a wide range in p_T .

The central assumption in forming the anti-particle to particle ratios is that the detector response is symmetric with respect to charge and therefore no corrections to the yields for the reconstruction efficiency or detector acceptance are required. However, losses due to the absorption of anti-protons in the detector material have the potential to modify the $\bar{\Lambda}/\Lambda$, $\bar{\Xi}^+/\Xi^-$ and $\bar{\Omega}^+/\Omega^-$ ratios and feed-down from the decay of heavier strange baryons can modify both the $\bar{\Lambda}/\Lambda$ and $\bar{\Xi}^+/\Xi^-$ ratios. Absorption causes the final state anti-proton from $\bar{\Lambda}$ decay to fail to be reconstructed more often than the proton from Λ decay. The size of this effect has been estimated and corrected for using a GEANT simulation of the detector. Absorption reduces the apparent $\bar{\Lambda}/\Lambda$ and $\bar{\Xi}^+/\Xi^-$ ratios by 1% and 0.2% respectively. The decaying anti-particles also have a larger absorption cross-section than their corresponding particles, but since they decay within a few centimeters, before most of the absorbing materials have been traversed, this correction is even smaller and is implicitly included in the numbers given above. The observed $\bar{\Lambda}/\Lambda$ includes feed-down contributions. The total Λ yield contains Λ originating from Ξ^- , Ξ^0 and Ω^- decays, estimated to be $27 \pm 6\%$ [26]. Their anti-particle decays similarly contribute to $\bar{\Lambda}$. Assuming that these feed-down contributions to Λ and $\bar{\Lambda}$ are in the ratio of the $\bar{\Xi}^+/\Xi^-$ measurement, we obtain an actual $\bar{\Lambda}/\Lambda$ ratio, which we quote, 0.05–0.015 lower than the observed value. The only feed-down contribution to the $\bar{\Xi}^+/\Xi^-$ comes from the $\Omega^- \rightarrow \Xi^- \pi^0$ channel with a 9% branching ratio and was therefore neglected. Two processes modify the K^+/K^- ratio. Feed-down of kaons from the decay $\phi \rightarrow K^+ K^-$ was estimated, using the measured ϕ/K ratio [27, 28], to reduce the apparent K^+/K^- ratio by 0.8% at $p_T = 0.4$ GeV/c and less than 0.3% above $p_T = 1$ GeV/c. Secondary interactions were studied using GEANT simulations of HIJING [29] events and were found to increase the measured ratio by 0.7%. These corrections were applied in producing the final ratio.

After the absorption correction the value of the $\bar{\Lambda}/\Lambda$ ratio is $0.74 \pm 0.01(stat.)$ in the measured acceptance interval of $p_T > 0.4$ GeV/c and within one unit of rapidity centered at mid-rapidity. This is the same as the value for the corrected data reported previously [26]. The feed-down correction reduces this to a final value of $0.71 \pm 0.01(stat.)$. The $\bar{\Xi}^+/\Xi^-$ ratio after correction is $0.83 \pm 0.04(stat.)$, measured over the same rapidity interval and $p_T > 0.5$ GeV/c. In order to admit a larger sample of Ω^- and $\bar{\Omega}^+$, the $\bar{\Omega}^+/\Omega^-$ ratio was calculated using a larger interval, of ± 1 units of rapidity, and a value of $0.95 \pm 0.15(stat.)$ was obtained. The $\bar{\Lambda}/\Lambda$ and $\bar{\Xi}^+/\Xi^-$ ratios as a function of p_T out to 2.5 GeV/c and 3.5 GeV/c are shown in Figure 2 and are consistent with a constant value. Within statistics the

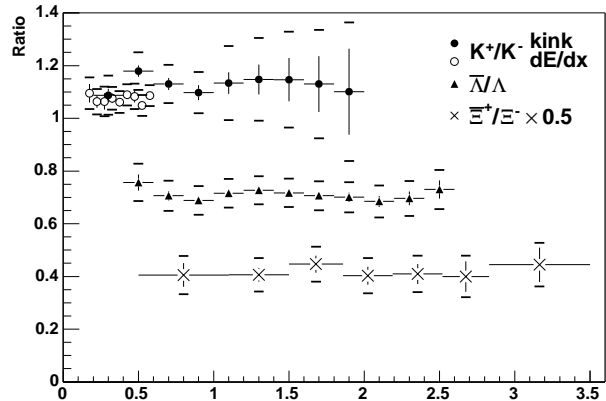


FIG. 2: The ratios $\bar{\Lambda}/\Lambda$, K^+/K^- and $\bar{\Xi}^+/\Xi^-$ as a function of p_T . The error bars indicate the statistical errors and the brackets the systematic uncertainties.

$\bar{\Lambda}/\Lambda$ ratio appears to be independent of the charged particle yield at mid-rapidity. Systematic uncertainties on the $\bar{\Lambda}/\Lambda$ and $\bar{\Xi}^+/\Xi^-$ of 0.04 and 0.05 respectively have been estimated by varying the cuts used to identify decay candidates. There were insufficient data to estimate the systematic uncertainty on the $\bar{\Omega}^+/\Omega^-$ this way so the $\bar{\Xi}^+/\Xi^-$ systematic uncertainty was used since the reconstruction methods are identical. The K^+/K^- ratio is $1.075 \pm 0.008(stat.)$, measured via the dE/dx method, in the range $0.15 < p_T < 0.6$ GeV/c and ± 0.4 units of rapidity around mid-rapidity. The same ratio measured by the kink method is $1.13 \pm 0.015(stat.)$ and extends out to 2 GeV/c in p_T . The systematic error of the kink measurement due to detector effects is estimated to be 0.05 and that for the dE/dx is estimated at 0.03. The small discrepancy in the K^+/K^- from the two methods is within the estimated systematic errors and a combined value of 1.092 ± 0.023 was calculated, following the method of the PDG [24] when combining results from different experiments. As Figure 2 shows, with both methods, the ratio shows no significant deviation from a constant as a function of p_T . As all the p_T intervals cover a large fraction of the total yield (over 70% [26, 28, 30]) we assume that the ratios we measure are a good indication of the ratios in the integrated yields.

The strange anti-baryon to baryon ratios are plotted in Figure 3 together with their values found in central Pb+Pb collisions at $\sqrt{s_{NN}} = 17$ GeV [31] at the CERN Super Proton Synchrotron. Also shown are the \bar{p}/p ratios from STAR [32] and two measurements at the lower energy from NA44 [33] and NA49 [34]. Figure 3 shows that the ratios increase with increasing strangeness content of the baryon at both $\sqrt{s_{NN}} = 17$ GeV and $\sqrt{s_{NN}} = 130$ GeV. The increasing trend in the ratios may be explained in a simple quark coalescence model [16, 17], which predicts that the anti-baryon to baryon ratios should be related to one another by a common multiplicative factor. The

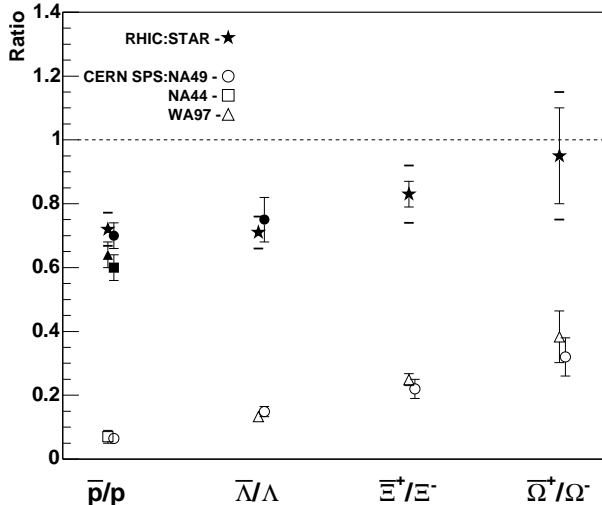


FIG. 3: Anti-baryon to baryon ratios measured by STAR and other RHIC experiments [35, 36, 37, 38], for baryons of increasing strangeness content, compared to values obtained in experiments [31, 33, 34, 39, 40, 41] at the SPS. For STAR points the bars indicate the statistical uncertainties and the brackets the additional systematic errors.

TABLE I: K^+/K^- ratio compared to compound ratios having the same net quark content. Comparisons made for this experiment and experiments at SPS [31, 33, 34, 39, 40, 41].

	STAR	SPS
K^+/K^-	1.092 ± 0.023	1.76 ± 0.06
$\frac{\bar{\Lambda}/\Lambda}{\bar{p}/p}$	0.98 ± 0.09	2.07 ± 0.21
$\frac{\bar{\Xi}^+/\Xi^-}{\bar{\Lambda}/\Lambda}$	1.17 ± 0.11	1.78 ± 0.15
$\frac{\bar{\Omega}^+/\Omega^-}{\bar{\Xi}^+/\Xi^-}$	1.14 ± 0.21	1.42 ± 0.22

multiplicative factor is given by the value of the K^+/K^- ratio. This is in approximate agreement with the data presented here, as shown in Table I.

Within the coalescence model hadrons are formed from a system of independent quarks and anti-quarks. An alternative description of particle production which nevertheless gives equivalent predictions for the ratios discussed here is the statistical model approach [42], which does not distinguish between quark or hadron degrees of freedom. In this case the multiplicative factor is $\exp(2\mu_B/3T - 2\mu_s/T)$, where μ_B is the baryon chemical potential, μ_s is the strange quark chemical potential and T is the chemical freeze-out temperature. The

K^+/K^- ratio can therefore be interpreted as an indirect measure of the baryon chemical potential. If the central region in Au+Au collisions at $\sqrt{s_{NN}} = 130$ GeV were net baryon free ($\mu_B = 0$), then the K^+/K^- ratio would be equal to one, and in both models the anti-baryon to baryon ratios would also be equal to one, under the assumption that strangeness is locally conserved. However, while the anti-baryon to baryon ratios at this higher energy are closer to unity, reflecting a lower net-baryon density, this density is nevertheless still positive. This is thought to be a consequence of baryon number transport (or stopping) during the collision process. There is an excess of u and d quarks over their anti-quarks favoring the production of baryons over anti-baryons and K^+ over K^- . We find, from a fit to all the ratios, that $\mu_B/T = 0.18 \pm 0.03$ and $\mu_s/T = 0.001 \pm 0.011$ with $\chi^2/dof = 2.5$ when including all the systematic errors. A statistical model analysis using preliminary data [43] is also consistent giving $\mu_B/T = 0.26 \pm 0.03$ where $\mu_B = 45$ MeV and $T = 170$ MeV. This compares to $\mu_B/T = 1.58 \pm 0.04$ at $\sqrt{s_{NN}} = 17$ GeV where $\mu_B = 266$ MeV and $T = 168$ MeV [12]. We also note that the flatness of the $\bar{\Lambda}/\Lambda$ and K^+/K^- ratios in Figure 2 suggests that the transverse momentum distributions of the particles and their anti-particles are very similar. The matching p_T distributions are especially interesting for the Λ and $\bar{\Lambda}$, since there may be different production mechanisms. The Λ are believed to have component due to associated production (e.g. $pp \rightarrow p\Lambda K$) by the incoming baryons.

In summary, we have reported strange anti-particle to particle ratios measured by the STAR experiment at mid-rapidity in the 11% most central Au+Au collisions at $\sqrt{s_{NN}} = 130$ GeV. The ratios indicate that a fraction of the net-baryon number from the initial system is present in the excess of hyperons over anti-hyperons at mid-rapidity. The ratios are consistent with simple quark counting models and with a statistical description of particle production which is governed by a common baryon chemical potential and chemical freeze-out temperature.

Acknowledgments

We wish to thank the RHIC Operations Group and the RHIC Computing Facility at Brookhaven National Laboratory, and the National Energy Research Scientific Computing Center at Lawrence Berkeley National Laboratory for their support. This work was supported by the Division of Nuclear Physics and the Division of High Energy Physics of the Office of Science of the U.S. Department of Energy, the United States National Science Foundation, the Bundesministerium fuer Bildung und Forschung of Germany, the Institut National de la Physique Nucleaire et de la Physique des Particules of France, the United Kingdom Engineering and Physical Sciences Research Council, Fundacao de Amparo a Pesquisa do Estado de Sao Paulo, Brazil, the Russian Ministry of Sci-

ence and Technology, the Ministry of Education of China, the National Natural Science Foundation of China, and

the Swiss National Science Foundation.

-
- [1] J.-P. Blaizot, Nucl. Phys. **A661**, 3 (1999).
 [2] H. J. Specht, Nucl. Phys. **A698**, 341 (2002).
 [3] H. Beker et al., Phys. Rev. Lett. **74**, 3340 (1995).
 [4] M. M. Aggarwal et al. (WA98), Phys. Rev. Lett. **85**, 3595 (2000).
 [5] R. Albrecht et al. (WA80), Phys. Rev. Lett. **76**, 3506 (1996).
 [6] E. Andersen et al. (WA97), Phys. Lett. **B449**, 401 (1999).
 [7] M. C. Abreu et al. (NA50), Phys. Lett. **B410**, 337 (1997).
 [8] M. C. Abreu et al. (NA50), Phys. Lett. **B477**, 28 (2000).
 [9] H. Appelshauser et al. (NA49), Eur. Phys. J. **C2**, 661 (1998).
 [10] S. Margetis et al. (NA49), Phys. Rev. Lett. **75**, 3814 (1995).
 [11] I. G. Bearden et al. (NA44), Phys. Rev. Lett. **78**, 2080 (1997).
 [12] P. Braun-Munzinger, I. Heppe, and J. Stachel, Phys. Lett. **B465**, 15 (1999).
 [13] P. Koch, Z. Phys. **C38**, 269 (1988).
 [14] P. Koch, B. Müller, and J. Rafelski, Phys. Rept. **142**, 167 (1986).
 [15] J. Rafelski and B. Müller, Phys. Rev. Lett. **48**, 1066 (1982).
 [16] A. Bialas, Phys. Lett. **B442**, 449 (1998).
 [17] J. Zimányi, T. S. Biró, T. Csörgő, and P. Lévai, Phys. Lett. **B472**, 243 (2000).
 [18] K. H. Ackermann et al. (STAR), Nucl. Phys. **A661**, 681 (1999).
 [19] C. Adler et al., Nucl. Instrum. Meth. **A470**, 488 (2001).
 [20] K. H. Ackermann et al. (STAR), Phys. Rev. Lett. **86**, 402 (2001).
 [21] M. Aguilar-Benitez et al., Z. Phys. **C50**, 405 (1991).
 [22] C. Adler et al. (STAR), Phys. Rev. Lett. **86**, 4778 (2001).
 [23] S. Margetis, K. Šafařík, and O. Villalobos Baillie, Ann. Rev. Nucl. Part. Sci. **50**, 299 (2000).
 [24] K. Hagiwara et al. (Particle Data Group), Phys. Rev. **D66**, 010001 (2002).
 [25] W. Deng, Ph.D. thesis, Kent State University (2002).
 [26] C. Adler et al. (STAR), Phys. Rev. Lett. **89**, 092301 (2002).
 [27] C. Adler et al. (STAR), Phys. Rev. **C65**, 041901 (2002).
 [28] C. Adler et al. (STAR) (2002), nucl-ex/0206008.
 [29] X.-N. Wang, Phys. Rept. **280**, 287 (1997).
 [30] J. Castillo et al. (STAR), J. Phys. **G28**, 1987 (2002).
 [31] E. Andersen et al. (WA97), J. Phys. **G25**, 171 (1999).
 [32] C. Adler et al. (STAR), Phys. Rev. Lett. **90**, 119903(E) (2003).
 [33] M. Kaneta et al. (NA44), J. Phys. **G23**, 1865 (1997).
 [34] S. V. Afanasiev et al. (NA49) (2002), nucl-ex/0208014.
 [35] K. Adcox et al. (PHENIX), Phys. Rev. Lett. **88**, 242301 (2002).
 [36] K. Adcox et al. (PHENIX), Phys. Rev. Lett. **89**, 092302 (2002).
 [37] I. G. Bearden et al. (BRAHMS), Phys. Rev. Lett. **87**, 112305 (2001).
 [38] B. B. Back et al. (PHOBOS), Phys. Rev. Lett. **87**, 102301 (2001).
 [39] S. V. Afanasiev et al. (NA49), Phys. Lett. **B538**, 275 (2002).
 [40] S. V. Afanasiev et al. (NA49) (2002), nucl-ex/0205002.
 [41] S. V. Afanasiev et al. (NA49) (2002), nucl-ex/0209002.
 [42] J. Letessier, A. Tounsi, and J. Rafelski, Phys. Lett. **B292**, 417 (1992).
 [43] P. Braun-Munzinger, D. Magestro, K. Redlich, and J. Stachel, Phys. Lett. **B518**, 41 (2001).